A Communication-Less Multimode Control Approach for Adaptive Power Sharing in Ship-Based Seaport Microgrid

Mutarraf, Muhammad Umair; Terriche, Yacine; Nasir, Mashood; Guan, Yajuan; Lien Su , Chun; Vasquez, Juan C.; Guerrero, Josep M.

A Communication-less Multi-mode Control Approach for Adaptive Power-Sharing in Ships-based Seaport Microgrid

Muhammad Umair Mutarraf, *Student Member, IEEE,* Yacine Terriche, *Member, IEEE,* Mashood Nasir, *Member, IEEE,* Yajuan Guan, *Member, IEEE,* Chun-Lien Su, *Senior Member, IEEE,* Juan C. Vasquez, *Senior Member, IEEE,* and Josep M. Guerrero, *Fellow, IEEE*

Abstract—The increase in greenhouse gas emissions from the transportation sector together with the continued depletion of fossil fuels in general has encouraged an increase in the use of energy storage systems and renewable energy sources at seaports and also on short route yachts and ferries. At present most seaports, particularly smaller ones, are not provided with cold-ironing facilities – shore based power facilities, which provide electric power to ships from the national grid. Because of the lack of cold-ironing facilities at most ports auxiliary diesel engines and diesel generators on ships must be kept operating and online while at berth to supply auxiliary loads of ship. To address these requirements, one possible solution would be to provide cold-ironing facilities at all ports. However, in many circumstances, this is not cost-efficient as a port might be far from the national grid. To overcome these limitations a seaport microgrid can be formed through the integration of multiple shipboard microgrids (SMG) with decentralized control together with a charging infrastructure that is located on-shore. This integration of multiple shipboard microgrids and port-based charging stations is termed as a ships-based seaport microgrid. Typically, power is shared among different microgrids using data communication techniques, which adds to the cost and the complexity of the overall system. This paper proposes a communication-less approach based on multi-mode, de-centralized droop control that enables power sharing among several SMGs in both charging and discharging modes based on the state of charge of battery banks – electric power is either supplied or consumed. The proposed approach would be potentially useful for future autonomous ships and also for islands where port electrification is either not technically feasible or an economically viable solution. A simulation and hardware-in-the-loop results are provided to verify the control robustness of the proposed control strategy.

Index Terms—shipboard microgrids, power-sharing, decentralized droop control, mobile cold-ironing, resource balancing.

I. INTRODUCTION

Trade in the European Union (EU) is highly dependent on seaborne transportation for both intra-EU as well as global connectivity [1]. Seaborne transportation is not only the most cost-effective form of transportation it also produces lower levels of greenhouse gas emissions in comparison with transportation through other modes, e.g. over land and airborne transportation [2]. Short sea shipping accounts for one-third of intra-EU trade, which is crucial to the economies of the island nations and territories of the EU [3]. At present, 37% of intra-EU trade and 90% of the external EU trade is carried out by ships [1]. Although there are clear benefits of using ships over land-borne or airborne transportation, emissions from the shipping sector are high and account for 2.2% of total global emissions, which is more than the emissions from any EU state [4]. By one measure up to 2% of these emissions take place at seaports [5]. It is anticipated that these emissions might increase by 150 to 250% by 2050 in comparison with 2008 levels if changes to how ships are powered in port are not introduced [6]. Any increase in seaborne trade in the coming years will very likely lead to an increase in the number of marine vessels operating in the EU, and hence, an increase in power demand during their berth-in-time results in an increase in emissions from these ships. This problem needs to be addressed through innovative ways [7].

Alternative power sources should be considered along with energy storage devices for both short route ships as well as for seaports. When fossil fuel-powered ships berth at the ports they produce emissions that are harmful to the population living close to these ports. One solution to the reduction of emissions from the seaports is addressed by providing power to ships from shore power connected to the national grid, which is known as cold-ironing. Although cold-ironing helps to minimize emission from ships at berth it ultimately increases the power demand on the national grid. Additionally, providing power to seaports that are far from the national grid could require huge investment costs, such as building infrastructure for electrification of seaports (power plants, transmission lines, substations, etc.) and therefore would not be deemed as a feasible solution. Alternatively, we propose a shipboard microgrid (SMG) having local power generation from renewable energy sources (RES) on ships, which at the same time having the ability to share power with the peer ships in port, effectively providing mobile cold-ironing facilities. This approach could be implemented using a public-private partnership or by providing incentives to shipowners who own battery-equipped yachts or ferries. It would not only help to

M. U. Mutarraf, Y. Terriche, M. Nasir, Y. Guan, J. C. Vasquez and J. M. Guerrero are with the Center for Research on Microgrids (CROM), Department of Energy Technology, Aalborg University, 9220 Aalborg East, Denmark (mmu, yte, mnas, ygu, juq, joz)@et.aau.dk.

C. L. Su is with the Department of Electrical Engineering, National Kaohsiung University of Science and Technology, Kaohsiung, Taiwan. (E-mail: cls@nkust.edu.tw)

minimize emissions from the transportation sector but would also create a sustainable solution involving ports and ship-owners to contribute to the blue growth (Europe's vision) [8].

The majority of the academic literature on this topic and existing implementations of solutions have focused on either SMGs [9], [10], [11], [12] or seaport microgrids [13]. A linkage between ports and ships is considered in [14] that emphasizes the ship-to-grid (S2G) concept where energy is transferred for the electrification of a remote island. However, from the search of existing literature that we conducted in choosing this topic, no existing studies have considered the operation of SMG for use as a potential mobile cold-ironing station. To connect loads with RES, power electronics-based converters are deployed. Parallel operation of DC-DC converters provides several benefits over an individual stand-alone converting units, as parallel operations provides recon-figurability, modular structure, redundancy, and fault tolerance [15]. The main challenge to the control system occurs when these converters are connected in parallel and reliability of a distributed system becomes highly dependent on the ability to share an equal amount of power during steady-states as well as during the transient states. Several approaches have been described in the literature, such as the centralized approach [16] where the central controller is used to provide the current reference to each converter. Another approach commonly utilized in literature is the master-slave approach [17] that guarantees all the slave modules to follow the current reference of the master. Yet another approach – circular chain control (3c) is proposed in [18], which states that all the modules have the same circuit configuration and each module has its own inner and outer loop control. In this approach, the modules are in a circular chain and each converter generates the reference of the current for the previous one. However, existing tradi-tional current-sharing approaches rely mostly on the physical connection of several converter modules that compromises the reconfigurability and redundancy of the system.

Traditional power/current-sharing methods pivot on equi-table power-sharing, which can result in battery banks with a lower state of charge (SoC) to degrade and, as a result of this, are not efficient. Because of these factors power-sharing based on droop control is proposed in [19] is attained by varying the droop coefficient accordingly with the SoC of battery banks. The study in [20] proposes proportional power-sharing for DC microgrids to attain power balancing between several distributed sources having different SoCs. These conventional approaches all make a trade-off between power/current-sharing accuracy and voltage regulation. To deal with these problems, the study in [21] proposes the SoC balancing approach in which the droop coefficient is set to be inversely proportional to the SoC^n in order to adjust the speed of SoC balancing. Although this approach does achieve resource balancing during discharging mode it unfortunately fails to provide proportional power-sharing in charging mode. Further, using this approach – single-mode droop – in ships-based seaport microgrids, results in unnecessary power-sharing that causes distribution losses for unwanted SoC balancing. In order to have proportional power/current sharing among different resources in both discharging and charging modes,

a multi-mode I-V droop method is proposed in [22]. This has the advantage in a way that the I-V droop method has a better transient performance in comparison with the V-I droop approach. However, stability margins for this approach are relatively smaller in comparison with the V-I droop method and may result in instability issues by adding up constant power loads [23], [24]. A simplified form of the multi-mode droop approach is proposed in [25], [26], [27] but extreme conditions were not tackled in these studies and stability analysis was ignored.

As a solution to the different problems of the control methods listed above, this paper proposes a multi-mode droop control to provide a decentralized power/current-sharing a-mong various SMGs. V-I droop control works in the region where SoC is between the minimum and maximum threshold limit, and that helps to enhance stability margins. In contrast, I-V droop mode operates in the region when SoC is below the minimum threshold limit or above the maximum threshold limit to enhance the transient response. In order to achieve resource balancing and using resources efficiently, instead of using fixed droop value, it is varied as a function of SoC. By applying such an approach, SMG with higher available resources will supply the highest current whereas the least current will be shared by the SMG having the lowest SoC.

A summary of this work can be addressed as follows:

1) A mobile cold-ironing approach for providing power to ships at berth, particularly for smaller remote islands where electrification of the seaport is not considered as a feasible/cost-effective solution.
2) A decentralized multi-mode adaptive droop control to achieve proportional power-sharing in both charging and discharging modes.
3) Small-signal analysis to support the stability of the proposed multi-mode algorithm.

The remainder of the paper is organized as follows: In Section II, the overall architecture of the ships-based seaport microgrids is described along with the adaptive droop control strategy. In order to know the behavior of the proposed scheme with small disturbances, a small-signal stability analysis is performed in Section III. To support the proposed approach, case studies are taken into account and are verified through simulation and experimental results in Section IV. The con-clusion is presented in Section V.

II. ARCHITECTURE FOR SHIPS-BASED SEAPORT MICROGRID

The overall architecture for the proposed ship-based seaport microgrid scheme is illustrated in Fig. 1. This architecture has the capability to provide both a mobile-cold ironing facility as well as enable capability to share power amongst ships. The architecture consists of several ships interfaced with RES and battery banks, which are interconnected with each other via charging stations placed onshore. These sources consist of battery banks (lithium-ion), solar panels, and fuel cell stacks. A cold-ironing facility based on DC distribution is used in this scheme as the output of most of the RES and energy storage systems (ESS) is a DC voltage, which

minimizes power conversion stages. The lack of reactive power compensation required in AC systems results in lower cost and higher efficiency.
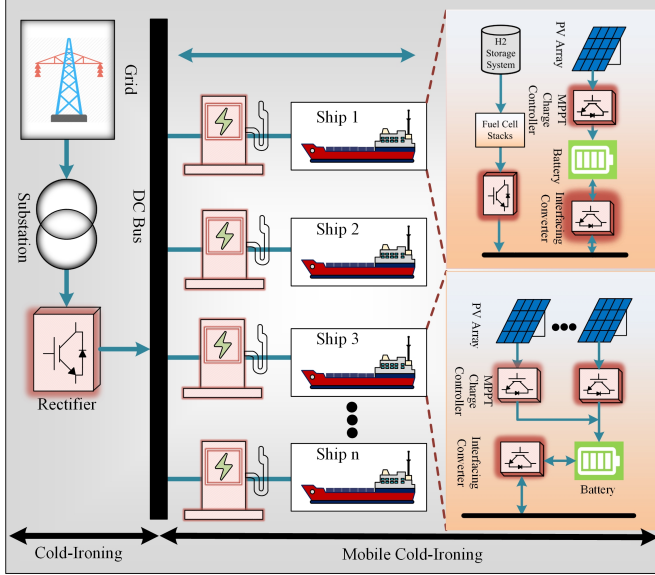

Fig. 1: A generic scheme of ships-based seaport microgrid [27].

A. Decentralized droop control algorithm

Multiple ships (yachts or ferries) are interconnected in parallel via charging stations onshore and any mismatch in the output voltage of the SMG will result in circulating current to flow between converters. Therefore, to diminish the flow of circulating current, droop resistance is added in the outer voltage loop, which can be expressed as follows:

$$V_{\text{o}} = V_{\text{ref}} - I_{\text{o}}R_{\text{D}}$$
$$R_{\text{D}} = \frac{\Delta V_{\text{D}}}{i_{\text{max}}} \tag{1}$$

where V_o and I_o are the output voltage and current respectively, V_{ref} is the reference voltage, R_D is the droop resistance, ΔV_D is the maximum allowable deviation, and i_{max} corresponds to the maximum output current. In the proposed approach each SMG is interfaced with RES, i.e., fuel cell stacks or photovoltaic (PV) and battery banks, and power is shared with the peer ships without using any communication connection. The droop value is varied based on the SoC of the battery banks and bus voltage V_o, and therefore, the current-sharing for each SMG depends on the SoC. The SoC of the battery banks can be estimated using the Coulomb counting method as expressed in (2).

$$SoC_\alpha(t) = SoC_\alpha(0) + \frac{1}{C_{bat}} \int_0^T V_0(I_{\text{in}} - I_{\text{L}})dt \tag{2}$$

where $SoC_\alpha(0)$ is the initial SoC and C_{bat} is the capacity of battery (Wh). V_o and I_{in} refers to the voltage of bus and the input current supplied by generation source (PV or fuel cell) respectively whereas I_L is the current supplied to DC bus.

To increase the lifetime of the battery, energy balancing along with optimal power-sharing is required. Power-sharing among various SMGs are classified into six modes depending on the SoC of battery banks. These modes are assigned as: variable current-controlled charging mode (VCCM), i.e., $0 \leq SoC_\alpha < SoC_{min}$, V-I droop mode ($SoC_{min} \leq SoC_\alpha < SoC_{max}$), variable current-controlled discharging mode (VCDM), i.e., $SoC_{max} \leq SoC_\alpha \leq 100$, and extreme conditions (Modes 1 and 6) as shown in Fig. 2. The maximum allowable upper (V_U) and lower (V_L) voltage deviation is set to be $\pm 5\%$ of the reference voltage (V_{ref}).

1) I-V Droop Mode–Modes 1 & 6: The first mode corresponds to a scenario where generation sources (PV and fuel cell) are unavailable and SoC of all SMGs are below the threshold limit, i.e., $0 \leq SoC_\alpha < SoC_{min}$, which will cause bus voltage to fall below the minimum allowable voltage deviation ($V_o < V_L$). In order to cope with this challenge, the constant I-V droop method is utilized such that to limit power-sharing upon such extreme conditions resulting in stabilizing DC bus voltage within allowable deviation. The reference current, in this case, can be found using (3).

$$I_{\text{ref}} = \frac{V_{\text{L}} - V_0}{R_{\text{D}}} \tag{3}$$

Similarly, in a scenario when abundant resources are available and SoC of all battery banks are above the maximum threshold limit, i.e., $SoC_\alpha > SoC_{max}$, such a scenario will result in an over-voltage condition ($V_o > V_U$), which destabilizes the whole system. To cater to this issue, power-sharing is limited based on the constant I-V droop method such that V_o is equivalent to V_U, the reference current for such a case can be calculated using (4).

$$I_{\text{ref}} = \frac{V_{\text{U}} - V_{\text{o}}}{R_{\text{D}}} \tag{4}$$

2) VCCM–Mode 2: The second mode corresponds to VCCM as shown in Fig. 2, this mode operates when SoC_α of SMG_i is below the minimum limit, i.e., $0 \leq SoC_\alpha < SoC_{min}$. The SMG in VCCM will start to consume power from peer SMGs until SoC_{min} is achieved. In such a scenario, bus voltage V_o will be greater than the V_L ($V_o \geq V_L$) indicating that only a few SMGs are deficient in resources. The reference current for such a case can be calculated using (5). By using such an approach SMG with the lowest SoC will absorb the highest current in comparison with SMG having higher SoC.

$$I_{\text{ref}} = I_{\text{rat}}\left(\frac{SoC_\alpha - SoC_{\text{min}}}{SoC_{\text{min}}}\right) \tag{5}$$

where I_{rat} is the rated output current.

3) V-I Droop Mode–Modes 3 & 4: Modes 3 and 4 operates in V-I droop mode, which corresponds to a case when SoC_α of the battery in certain SMG is above the minimum set value and below the maximum set threshold value ($SoC_{min} \leq SoC_\alpha < SoC_{max}$). The droop value for such a mode upon charging and discharging can be calculated using (6)–(7) respectively. When all SMGs are in V-I droop mode, it shows that they are self-sufficient such that ships can run their internal loads in isolation, power-sharing is not required. This avoids redundant
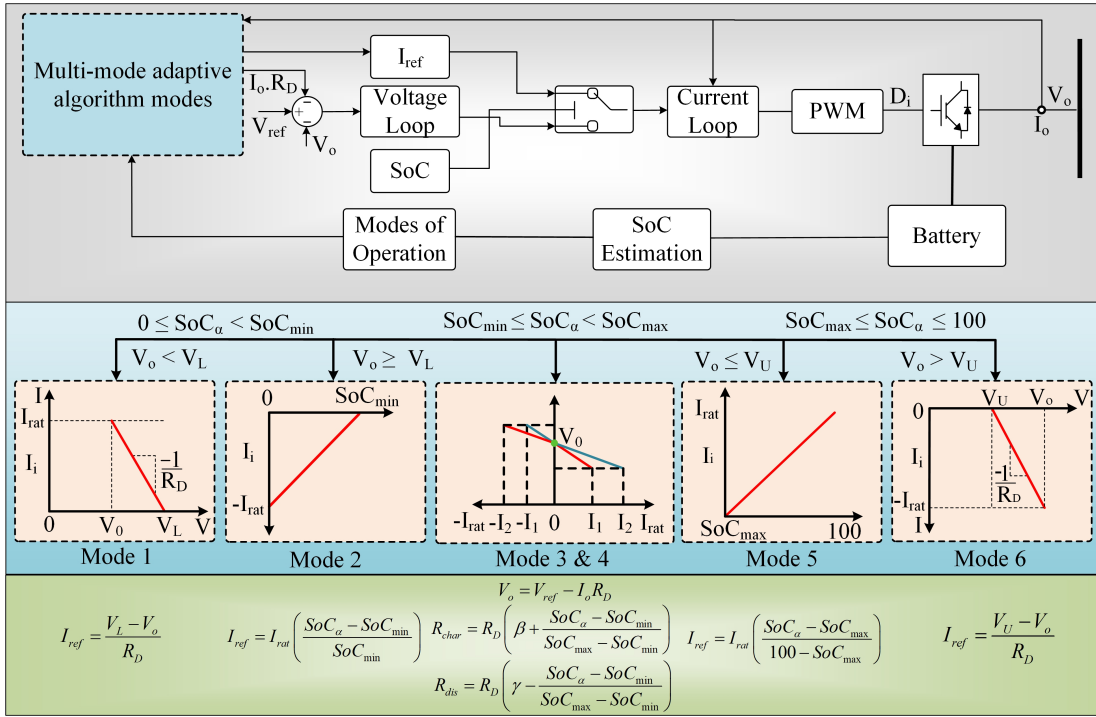
Fig. 2: Multi-mode adaptive droop control algorithm.

distribution losses, therefore when all the ships have self-sufficient power the adaptive algorithms adopt (Modes 3 & 4) to ensure zero power-sharing. If a new diesel-equipped ship arrives at the port and requires connection with the mobile cold-ironing facility to power its auxiliary load, peer SMGs based on their available resources will share the power such that SMG with lower SoC shares the least power as soon as the ship is connected.

$$R_{\text{char}} = R_D(\beta + \frac{SoC_\alpha - SoC_{\min}}{SOC_{\max} - SoC_{\min}}) \qquad (6)$$

$$R_{\text{dis}} = R_D(\gamma - \frac{SoC_\alpha - SoC_{\min}}{SoC_{\max} - SoC_{\min}}) \qquad (7)$$

where R_D is the droop resistance, $\beta = 1$ and $\gamma = 2$ are the droop coefficients. Droop resistance (R_D) is varied linearly from R_D to $2R_D$ and hence these values are calculated in this manner.

4) VCDM–Mode 5: The last mode corresponds to VCDM as illustrated in Fig. 2. This is a case when the SoC is above the maximum limit, i.e., $SoC_\alpha > SoC_{max}$ and $V_o \leq V_U$. In such a scenario SoC of some SMGs has the value above SoC_{max}, which shows that they are sufficient in their resources and generation by RES than can be used to charge the batteries of the nearby ships. The current reference for such a scenario can be calculated using (8). By using such an approach, the SMG with the highest SoC will supply the highest current in comparison with SMG having the lowest SoC.

$$I_{\text{ref}} = I_{\text{rat}}(\frac{SoC_\alpha - SoC_{\max}}{100 - SoC_{\max}}) \qquad (8)$$

III. SMALL-SIGNAL STABILITY ANALYSIS

Small-signal stability analysis is performed to verify the stability of power electronic-based converters when experiencing small disturbances. For instance, if a converter is subjected to small disturbances that cause deviation in the system variables for a longer period, the power system still remains stable. Generally, a charging station for an electric ship is comprised of several stages as the power is supplied from the grid and hence, AC to DC conversion stage is needed. For our case owing to have DC SMGs, we, therefore, required only a DC-DC conversion stage. There are several DC-DC converter topologies used in the literature, in order to implement our proposed method, we have taken into consideration here the synchronous buck converter since it is simple, efficient, and reliable. The block diagram of a simplified form of a buck converter with dual-loop control, i.e., inner current, and outer voltage-loop along with the droop control is shown in Fig. 3. The varying droop resistance is inversely proportional to the SoC of the battery, hence, changing the droop resistance varies the SoC of the battery [28].
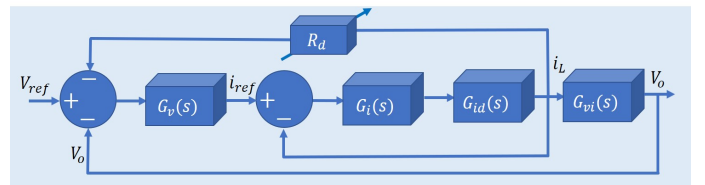

Fig. 3: Block diagram of the control system for single SMG [28].

The mathematical model of an average buck converter

model is described by expression (9)–(10).

$$L\frac{di_L}{dt} = DV_g - V_o - i_L R_{SR} \qquad (9)$$

$$C\frac{dV_C}{dt} = i_L - \frac{V_o}{R_L} \qquad (10)$$

where V_g is the input voltage, V_o is the output voltage, D is the duty-cycle, C, L, R_{SR}, and R_L shows capacitance, inductance, stray resistance of the converter, and load attached at the output respectively. The overall transfer function of a dual-loop control of buck converter can be expressed as shown in (11).

$$\frac{V_o}{DV_g} = \frac{1}{LCs^2 + (R_{SR}C + \frac{L}{R_L})s + (1 + \frac{R_{SR}}{R_L})} \qquad (11)$$
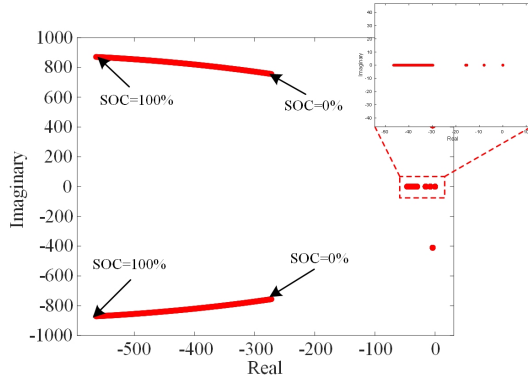
(a) Impact of varying SoC on the stability.
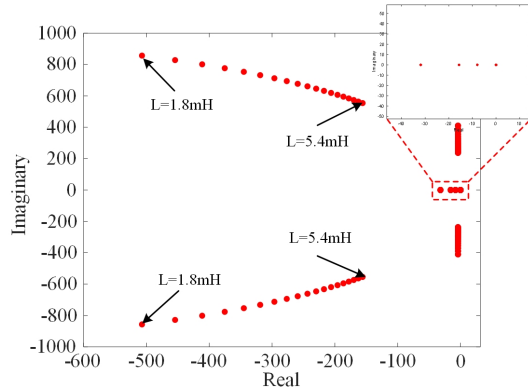
(b) Impact of varying inductance on the stability.

Fig. 4: Closed-loop eigenvalues for the system.

The control system illustrated in Fig. 3 is investigated with parameters: V_g = 320V, V_o = 220V, P = 2.2kW, R_D = 0.76 − 4.56Ω (0 to 100% SoC), L = 1.8 − 5.4 mH , SoC_{min} = 30%, SoC_{max} = 80%, sampling time (0.0001s), C = 3300μF and R_{SR} = 0.2Ω. The charging stations for ships vary from several kW to MW range but the choice of power level in the current work, i.e. 2.2 kW, is primarily made due to the maximum rating of the power converter available in the laboratory (Danfoss converter 2.2 kW) used as a reference. It can be observed from Fig. 4

(a) that during charging mode (increasing SoC) the poles start moving towards the left in the left half of the s-plane, which shows that system is moving towards a more stable region while keeping L constant, i.e., $1.8mH$. On the other hand, during discharging mode the droop value decreases, and hence, poles start moving towards the right. Similarly, keeping droop resistance constant (3.8Ω) and changing the inductance $(1.8mH$ to $5.4mH)$ varies eigenvalues as shown in Fig. 4 (b). It is observed that by increasing the inductance, poles start to move towards an unstable region.

Multiple SMG's are connected such that power is shared among them by varying the droop resistances based on the SoC of the battery banks by varying the droop resistances. Hence, each SMG can either absorb or inject power to and from the other SMG. In order to verify the impact of variations in the parameters on the stability of the overall system, power-sharing among two SMG's that are connected via a tie-line impedance is considered as illustrated in Fig. 5 where G_{id} and G_{vi} is defined in (12). Similarly, such a model can be further extended to verify the stability for multiple SMG's.

$$G_{id} = \frac{V_{in}}{R_L} \frac{1 + sR_LC}{LCs^2 + (R_{SR}C + \frac{L}{R_L})s + (1 + \frac{R_{SR}}{R_L})}$$
$$G_{vi} = \frac{R_L}{1 + sR_LC} \qquad (12)$$

The state-space model is derived from the model in order to know the behavior of the system upon variation in SoC of battery banks and inductances. In the first scenario, we have considered Mode 3 and several possible eigenvalues are generated for the variations in SoC of SMG_1 from 31 to 55% and variations in SoC of SMG_2 from 58 to 79% by keeping inductance constant, i.e., $1.8mH$. It can be verified from Fig. 6 (a) that if the battery banks are being charged (increasing SoC) the eigenvalues in an s-plane start moving towards the further left side in a left-half plane, which shows the system's stability is enhanced. On the other hand by varying SoC of SMG_1 (31 to 55%) and SMG_2 (58 to 79%) along with varying inductance from $1.8mH$ to $5.4mH$ the poles start moving towards the right side as shown in Fig. 6 (b).

The small-signal stability analysis for a scenario when SMG_1 is in VCCM ($0 \leq SoC_\alpha < SoC_{min}$ and $V_o \geq V_L$) corresponding to Mode 2 whereas SMG_2 in V-I droop mode ($SoC_{min} \leq SoC_\alpha < SOC_{max}$) corresponding to Mode 3 is illustrated in Fig. 7. Although, in general, we do not deep discharge batteries, in order to consider the worst-case scenario, we have taken the whole possible window (0 to 29 %). Hence, the SoC for SMG_1 is varied from 0 to 29% and SoC for SMG_2 is varied from 31 to 79%, it can be observed from Fig. 7 that the system remains stable owing to have all poles in the left half-plane. The single loop in VCCM helps for faster transient response in comparison with dual-loop control.

IV. CASE STUDIES

To validate the proposed adaptive droop approach, various case studies are taken into consideration for simulation results, which are performed in MATLAB/SIMULINK environment and experimental results in form of hardware-in-the-loop
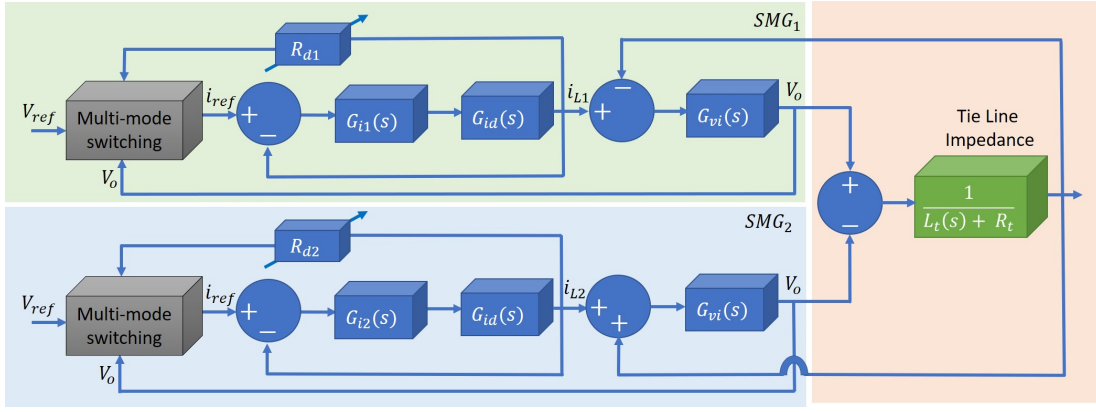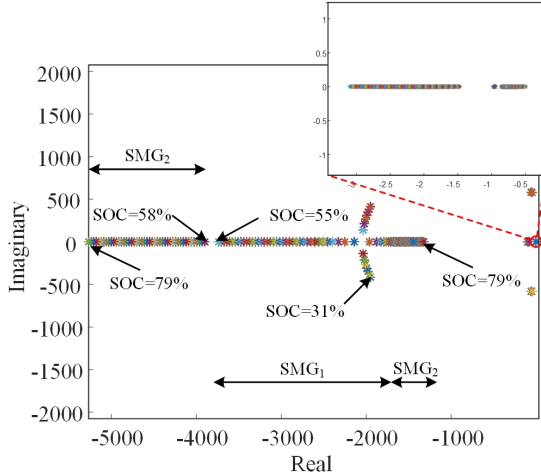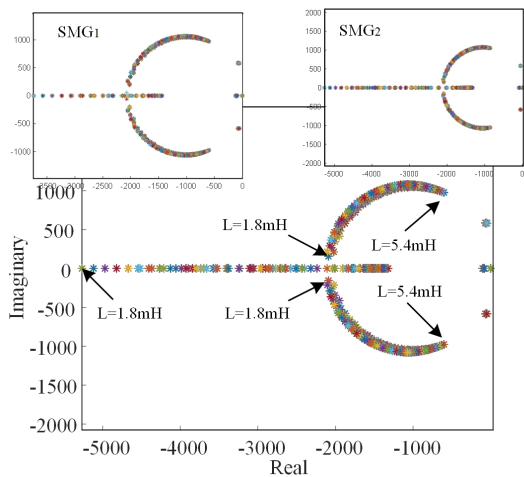
Fig. 5: Block diagram of the control system for two interconnected SMG's.

(HIL). Based on the size of the ship, the power levels of charging stations vary from a few kW to MWs range, while, the distribution voltage level is generally in the low voltage (LV) category.

(a) Impact of varying SoC.

(b) Impact of varying inductance.

Fig. 6: Eigenvalues for two interconnected SMGs.

To verify the proposed approach in a laboratory-scaled

environment and keeping hardware results consistent with the simulation results, we have scaled down parameters as shown in Table I. In this study, four SMGs are taken into account, which are interfaced in parallel by using a charging infrastructure comprising of a bi-directional converting unit thus forming a DC bus. The choice of DC bus voltage in the current work, i.e., 220V, is primarily made for demonstration and validation only. This voltage level was, however, also adopted in some of earlier navy ships [29]. Similarly, regarding power levels, the maximum rating of the power converter available in the laboratory (Danfoss converter 2.2 kW) was used as a reference. The scheme is equally valid for relatively high power and high voltage parameters.
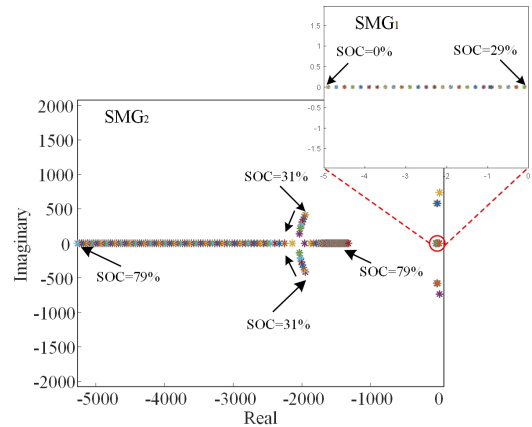

Fig. 7: Eigenvalues for two interconnected SMGs (Modes 2 & 3).
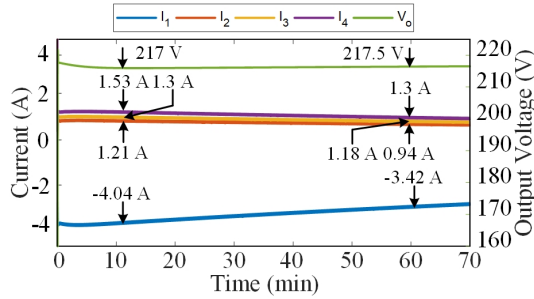
A. Simulation results

Several cases are taken into consideration and simulation results are performed in a MATLAB/Simulink environment to verify the proposed decentralized multi-mode droop control.

1) Case 1: When one of the SMG is in VCCM: The case when one of the SMG is lacking in resources such that the SoC of battery banks in this case is below the minimum threshold limit, i.e., $0 \leq SoC_\alpha < SoC_{min}$ whereas the rest of SMGs are within minimum and maximum threshold limits. In such a scenario the SMG having lower SoC than the minimum set

limit begins to consume power from the nearby ships as shown in Fig. 8. The SoC of battery in each SMG in this case are assumed to be $SoC_1 = 5\%$, $SoC_2 = 50\%$, $SoC_3 = 65\%$, and $SoC_4 = 79\%$. It can be further illustrated from Fig. 8 (a) that SMG_1 starts absorbing power from nearby SMGs in a way that SMG with higher SoC (SMG_4) supplies the highest power in comparison with SMG having lower SoC. As one of the SMGs is in VCCM and hence, V_o is less than the V_{ref}. Moreover, it can be observed from Fig. 8 (b) that SoC of SMG_4 declines the most owing to have the highest SoC.

TABLE I: Parameters for ships-based seaport microgrid.

Parameters	Value	Symbol
No of SMGs	4	n
DC Bus Capacitance	3300 μF	C
Voltage of DC bus	220 V	V_{ref}
Battery Voltage	320 V	V_g
Inductance of each converter	3.6mH	L
Rated power of converter	2.2kW	C_c
Rated power of PV panels	1 kW	P_{PV}
Rated power of FC	5 kW	P_{FC}
Switching frequency	10 kHz	f_{sw}
Battery Capacity in each SMG	15 kWh	C_B
Rated charging current	5A	I_{rat}
Minimum SoC threshold limit	30%	SoC_{min}
Maximum SoC threshold limit	80%	SoC_{max}
Droop resistance	1.9Ω	R_D

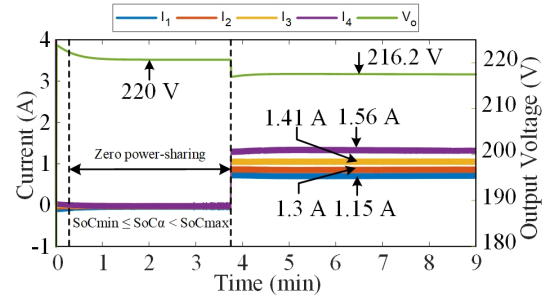(a) DC-bus voltage and current-sharing among SMGs.
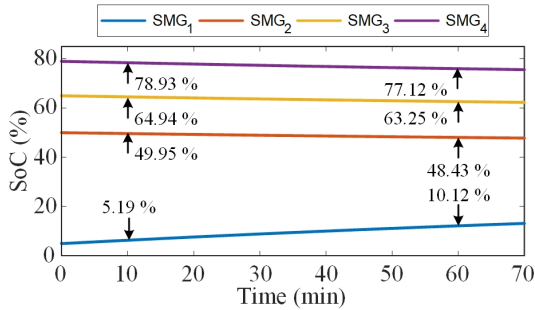
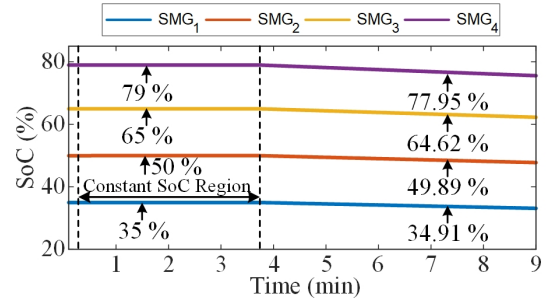(b) SoC of battery banks in different SMGs.

Fig. 8: Simulation results for the VCCM.

2) Case 2: When entire SMGs are in V-I droop mode: The second scenario corresponds to when entire interfaced SMGs are above the minimum set limit (SoC_{min}) and below the maximum set limit (SoC_{max}), i.e., $SoC_{min}\leq SoC_\alpha < SoC_{max}$. In such a case, all SMGs are self-sufficient

indicating that there will be zero power-sharing. Each ship can run its internal loads indigenously, power-sharing is not required. To avoid redundant distribution losses when all the ships have self-sufficient power the adaptive algorithms adopt (Modes 3 & 4) to ensure zero power-sharing. The SoC of battery for individual SMGs in this case are assumed to be $SoC_1 = 35\%$, $SoC_2 = 50\%$, $SoC_3 = 65\%$, and $SoC_4 = 79\%$. It can be verified from Fig. 9 (a) that the current-sharing between SMGs is zero and hence SoC of each battery bank in SMGs remains constant as shown in Fig. 9 (b). Moreover, owing to have zero power-sharing, the bus voltage will remain constant and is equal to the reference voltage, i.e, 220 V. At 3.75 mins, another ship, which is required with mobile cold-ironing facility connects with the main bus, each SMG starts to share power in accordance with their SoC such that SMG with lowest SoC supplies the least current as shown in Fig. 9 (a).
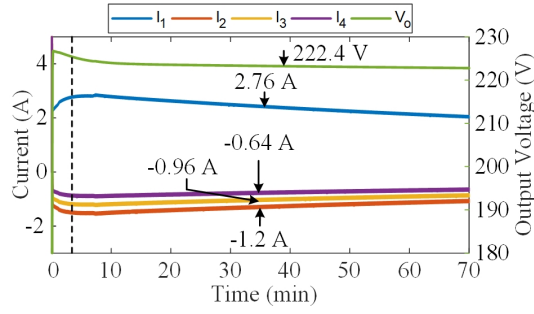

(a) DC-bus voltage and current-sharing among SMGs.

(b) SoC of battery banks in different SMGs.

Fig. 9: Simulation results for a V-I droop mode.

3) Case 3: When one or more of SMGs are in VCDM: Another scenario when one or more of SMGs are abundant in resources such that SoC of one or more of the SMGs are above the maximum set limit (SoC_{max}), i.e., $SoC_\alpha > SoC_{max}$ is considered here, in such a scenario, V_o is greater than V_{ref} ($V_o > V_{ref}$) as shown in Fig. 10 (a). The SoC of battery for individual SMGs in this case are assumed to be $SoC_1 = 95\%$, $SoC_2 = 35\%$, $SoC_3 = 50\%$, and $SoC_4 = 75\%$. Since SMG_1 is abundant in recourses, it starts to supply power with the peer ships whereas SMG_2 owing to have the lowest SoC absorbs the highest current as illustrated in Fig. 10 (a). As soon as the SoC reaches up to the maximum set value (SoC_{max}), there will be zero power-sharing. Further, it is verified from Fig. 10 (b) that SMG with lower SoC absorbs the highest current and its SoC inclines the most.

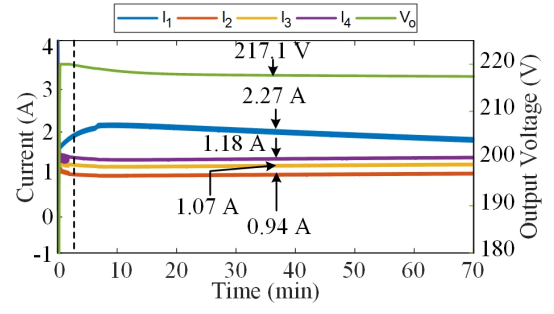(a) DC-bus voltage and current-sharing among SMGs.
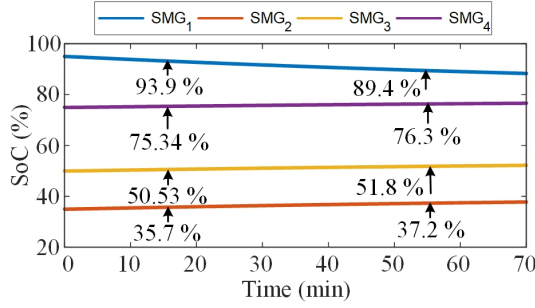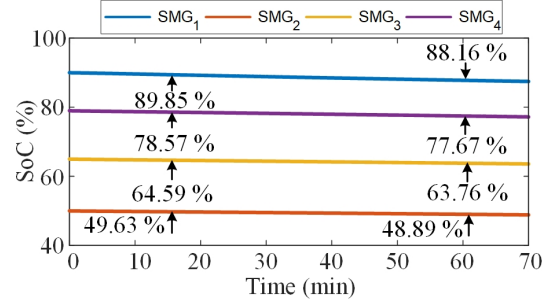

(b) SoC of battery banks in different SMGs.

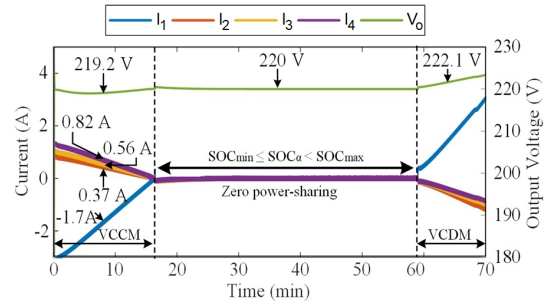Fig. 10: Simulation results for the VCDM.

(a) DC-bus voltage and current-sharing among SMGs.
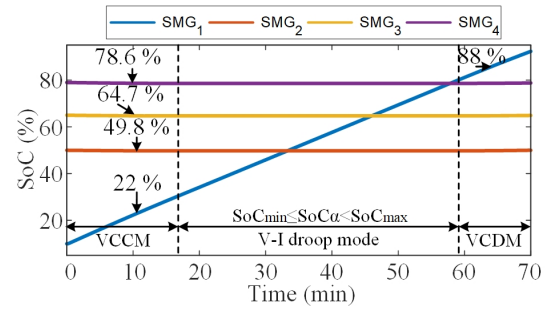

(b) SoC of battery banks in different SMGs.

Fig. 11: Simulation results for VCDM case with mobile cold-ironing facility.

Similarly, power-sharing for a scenario when one of the SMG has plenty of available resources, another one is required with a mobile-cold ironing facility, whereas the rest of the SMGs are within the minimum and maximum range is illustrated in Fig. 11. Since the SoC of SMG_1 is above SoC_{max}, hence, it will operate in VCDM. In such a scenario, SMG with SoC higher than SoC_{max} shares the current in accordance with the expression (8). It can be seen from Fig. 11 (a) that SMG_1 shares the highest current owing to have the highest SoC, i.e., 90% whereas the rest of the SMGs being in V-I droop mode shares current accordingly. Further, Fig. 11 (b) verifies that SoC of SMG_1 declines the most.

4) Case 4: Inter-mode transition: To visualize the transition from one mode to another, the SoC of the SMG_1 is considered below the minimum threshold value whereas the SoC of other SMGs is set above the minimum threshold limit. As SMG_1 is deficient in resources, other SMGs will share the current to charge their batteries to a minimum threshold value such that batteries with higher SoC provide current-sharing the most as illustrated in Fig. 12 (a). Further, power from the PV panels will continue to charge the batteries along with power shared by nearby SMGs. The DC bus voltage starts to rise and reaches the reference value as soon as all the SMGs become self-sufficient as shown in Fig. 12 (b). The initial SoC set for SMGs are 10%, 50%, 65%, and 79%. After the initial transient period, $SMG_2 - SMG_4$ starts to share the power with SMG_1 such that the SoC of SMG_1 reaches the minimum threshold value. After that there will be a region where there will be zero power-sharing, i.e., $SoC_{min} \leq SoC_\alpha < SoC_{max}$, hence, a constant region starts such that the DC bus voltage reaches the reference value. During this period PV panels in SMG_1 keep on charging battery banks. As soon as SoC of SMG_1 reaches above the maximum threshold limit, the VCDM starts.

At this stage, SMG_1 starts sharing extra power with nearby ships by providing power following the SoC of each SMG.

(a) DC-bus voltage and current-sharing among SMGs.

(b) SoC of battery banks in different SMGs.

Fig. 12: Simulation results for inter-mode transition mode.

5) Case 5: Extreme Conditions: A scenario when generation sources (PV & Fuel cell) are unavailable and SoC of all SMGs are below the set limit, i.e., $0 \leq SoC_\alpha < SoC_{min}$

may cause DC bus voltage to fall below the maximum lower deviation limit (V_L) and instigate instability in the whole system. To cope with this challenge in an extreme scenario I-V droop mode is taken into account, which limits current-sharing among different SMGs resulting in stabilizing DC bus voltage up to a value equivalent to V_L (lower threshold of voltage) while limiting any further power-sharing or load fulfillment. To verify it, initial SoC of battery banks, in this case, are assumed to be $SoC_1 = 5\%$, $SoC_2 = 15\%$, $SoC_3 = 20\%$, and $SoC_4 = 25\%$. It can be observed from Fig. 13 (a) that owing to have zero power-sharing, the SoC of all SMGs remains constant and the bus voltage remains equivalent to V_L. Similarly, another possibility when the SoC of all SMGs is above the maximum threshold limit, i.e., ($SoC_\alpha \geq SoC_{max}$) causes an overvoltage in the DC bus (V_o). It illustrates that batteries are charged, and excessive generation is available due to which the bus voltage may rise above the threshold, if not properly controlled. Hence, to stabilize the DC bus within the maximum allowable upper threshold limit (V_U) power-sharing among different SMGs will be limited by the I-V droop method. To verify this approach, the initial SoC of battery banks in this case are assumed to be $SoC_1 = 85\%$, $SoC_2 = 90\%$, $SoC_3 = 95\%$, and $SoC_4 = 100\%$. This sort of strategy will help to stabilize DC link voltage resulting in bus voltage equivalent to the maximum possible upper voltage deviation limit (+5% of reference voltage). It can be verified from Fig. 13 (b) that bus voltage remains constant, which is equivalent to the maximum possible deviation, i.e., 231 V and SoC of all SMGs remains constant. Further, in case of excessive generation by PV in this scenario will be curtailed to stabilize the whole system.
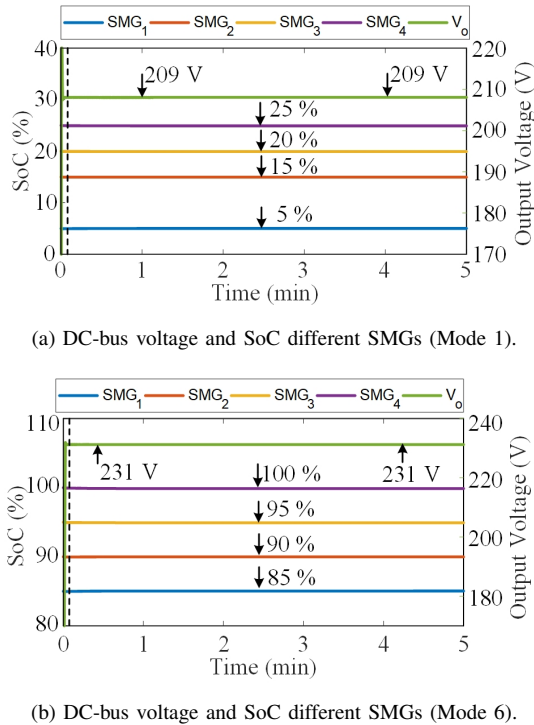

(a) DC-bus voltage and SoC different SMGs (Mode 1).

(b) DC-bus voltage and SoC different SMGs (Mode 6).

Fig. 13: Simulation results for extreme conditions.

6) Case 6: Comparison with traditional adaptive droop technique: The main goal of the adaptive droop technique

proposed in our approach and the one proposed in [21] is to achieve resource balancing. Although, the conventional adaptive approach utilized in [21] helps in proportional power-sharing during discharging mode but fails to achieve in charging mode. Alternatively, the proposed approach proportionally shares power in both charging and discharging modes. Consider two SMGs connected in parallel where the SoC of the SMG_1 is 40% and the SoC of the SMG_2 is 50%, which is supplied by a current-controlled source. The symbols I_1, I_2, SMG_1, SMG_2 illustrated in Fig. 14 are assigned to show the proposed approach whereas I_3, I_4, SMG_3, SMG_4 are used to show the approach utilized in [21]. It can be verified from Fig. 14 (a) that during charging mode, the adaptive droop technique proposed in [21] fails to provide proportional power-sharing and hence resources are not balanced. Due to this, the difference between SMG_3 and SMG_4 keeps on increasing, on the other hand, using our approach, the difference between SoC_1 and SoC_2 decreases, hence, verifying proportional power-sharing as illustrated in Fig. 14 (b).

(a) Current-sharing among SMGs.
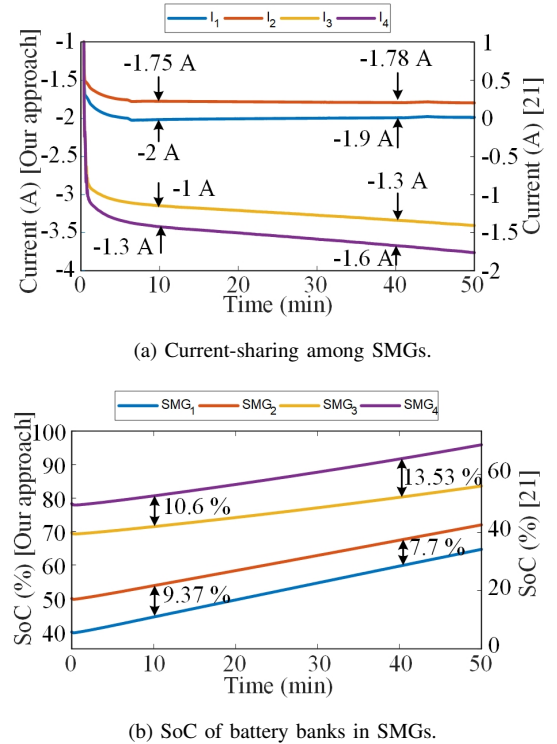

(b) SoC of battery banks in SMGs.

Fig. 14: Comparison using our approach and the one proposed in [21].

Similarly, proportional power-sharing during charging is achieved in other modes in the proposed scheme. Consider two SMGs connected in parallel where the SoC of the SMG_1 is 15% and the SoC of the SMG_2 is 25%, which is supplied by a current-controlled source. During charging mode, if we utilize the adaptive droop technique proposed in [21], a battery with higher SoC (SMG_2) will absorb more power in comparison to the battery with lower SoC (SMG_1) as depicted in Fig. 15 (a) and hence, resource balancing will not be achieved. Whereas in the proposed adaptive droop control, SMG with lower SoC

(SMG_1) will absorb more power, and hence, SoC of SMG_1 will rise more as shown in Fig. 15 (b).
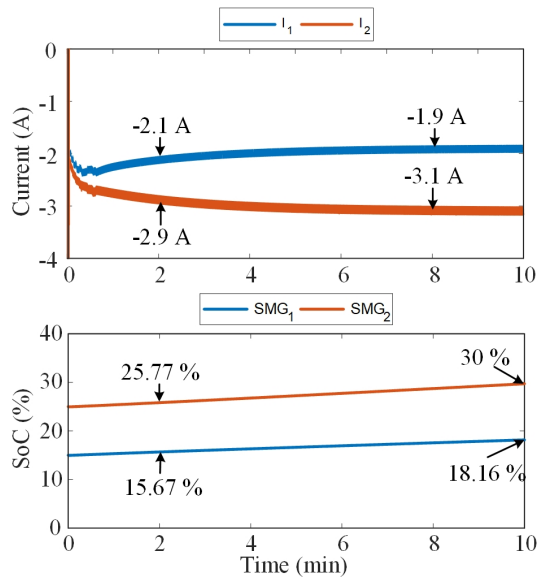
(a) Current-sharing and SoC of different SMGs using scheme proposed in [21].
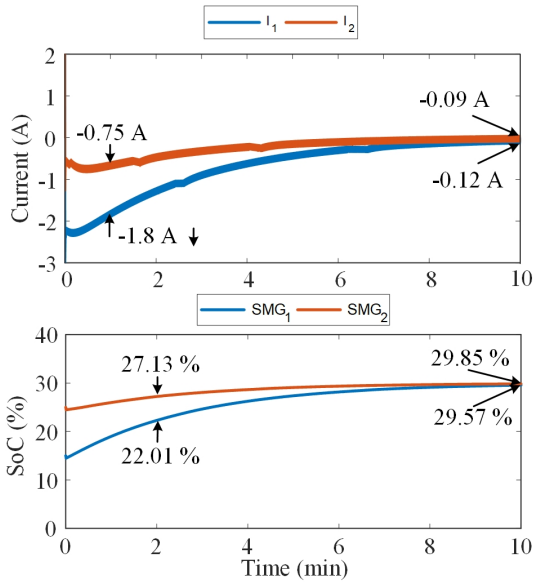
(b) Current-sharing and SoC of different SMGs using the proposed scheme.

Fig. 15: Simulation results for comparison between proposed adaptive droop with traditional approach.

B. Hardware-in-the-loop results

To verify the simulation results of several case studies presented above, the proposed multi-mode droop algorithm along with mobile cold-ironing facility is verified experimentally using the dSPACE 1006 platform for real-time control as shown in Fig. 16.

1) Case 1: When one of the SMG is in VCCM: The HIL results for a case when one of the SMG is in VCCM and the rest are in the range $SoC_{min} \leq SoC_{\alpha} < SoC_{max}$ are shown in
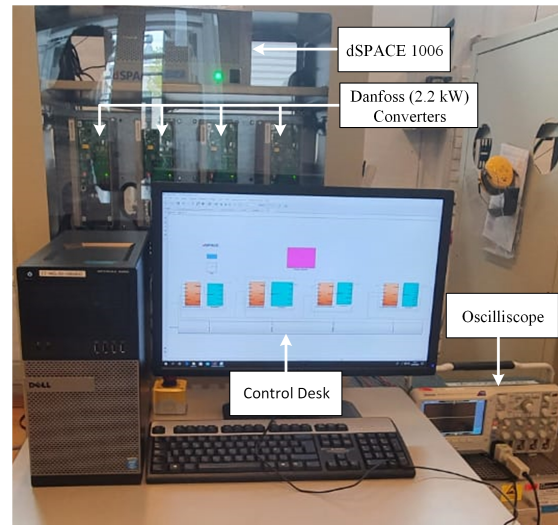

Fig. 16: Laboratory scaled setup for the proposed approach.

Fig. 17. The initial SoC of battery banks in each SMG in this case are assumed to be $SoC_1 = 5\%$, $SoC_2 = 50\%$, $SoC_3 = 65\%$, and $SoC_4 = 79\%$. Since SMG_4 is having the highest SoC due to which the current sharing for this SMG will be more than other SMGs as illustrated in Fig. 17 (a). Further, it can be seen from Fig. 17 (b) that SMG_1 is below the SoC_{min}, hence, it starts to absorb power from nearby SMGs. As soon as other SMGs start sharing power with SMG_1, its SoC starts to rise whereas the SoC of the rest of SMGs keep on declining as they are supplying power.
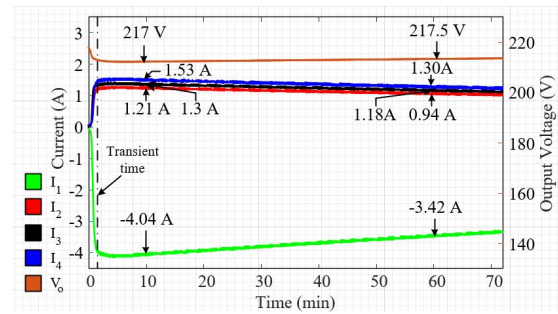
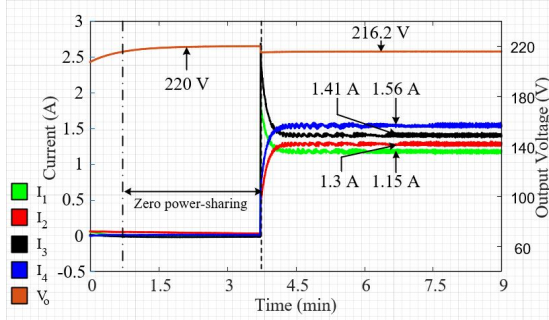(a) DC-bus voltage and current-sharing among SMGs.
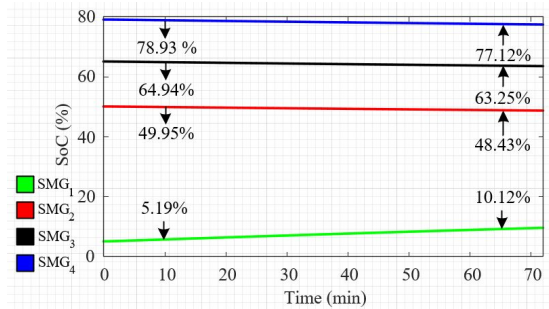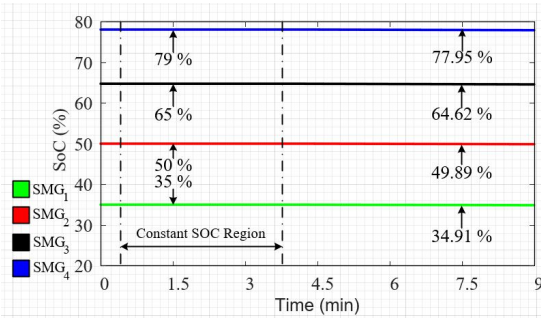

(b) SoC of battery banks in SMGs.

Fig. 17: Experimental results for the case study 1.

2) Case 2: When all SMGs are in V-I droop mode: Another scenario when all SMGs are in V-I droop mode, i.e., $SoC_{min} \leq SoC_{\alpha} < SoC_{max}$, in such a case there will not be any power-
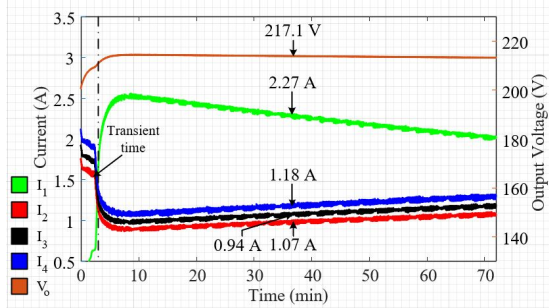
sharing as illustrated in Fig. 18.

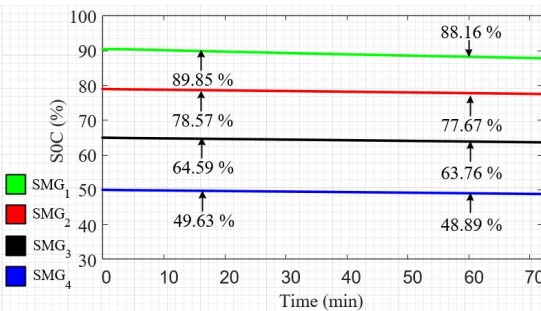(a) DC-bus voltage and current-sharing among SMGs.

(b) SoC of battery banks in SMGs.

Fig. 18: Experimental results for the case study 2.

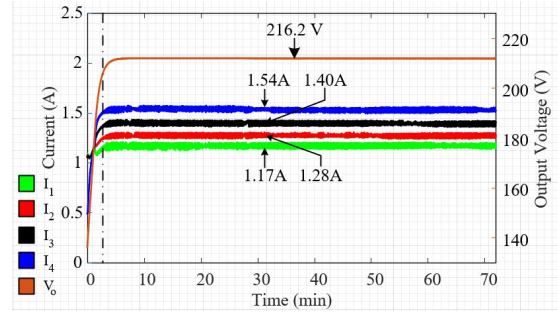(a) DC-bus voltage and current-sharing among SMGs.

(b) SoC of battery banks in SMGs.

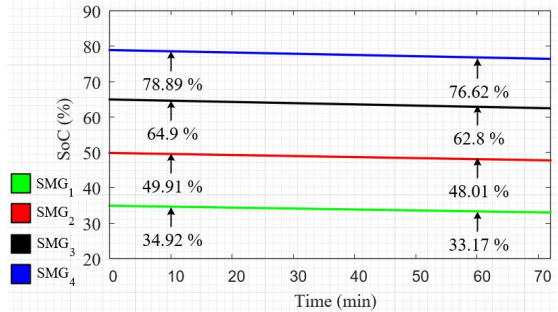Fig. 19: Experimental results for the case study 3.

It can be observed from Fig. 18 (a) that up till 3.7 $mins$ there is zero power-sharing such that V_o is equal to V_{ref} and hence SoC of battery banks in all SMGs remains constant. The initial SoC of battery banks in each SMG, in this case, are assumed to be $SoC_1 = 35\%$, $SoC_2 = 50\%$, $SoC_3 = 65\%$, and

$SoC_4 = 79\%$. At 3.7 $mins$ one of a diesel-based ship berthed at the seaport and is required with the mobile cold-ironing facility, SMGs will start to share the power in accordance with their respective SoC such that SMG_4 having higher SoC shares the highest current (I_4) whereas SMG_1 being lowest, shares the least current (I_1) as illustrated in Fig. 18 (a). Further, it can be observed from Fig. 18 (b) that SoC of SMG_1 and SMG_4 decreases the least and most respectively such that all resources are efficiently used and SoC balancing will be achieved.

3) Case 3: When one of the SMG is in VCDM: A case when one of the SMG is abundant in resources such that the SoC of this SMG is above the maximum threshold limit, i.e., $SoC_\alpha \geq SoC_{max}$ is considered here. The initial SoC of battery banks in each SMG in this case are assumed to be $SoC_1 = 90\%$, $SoC_2 = 79\%$, $SoC_3 = 65\%$, and $SoC_4 = 50\%$. To verify experimentally, we have taken into account that SMG_1 is in VCDM whereas the rest of SMGs are in V-I droop mode providing a mobile cold-ironing facility. It can be verified from Fig. 19 (a) that SMG_1 owing to be in VCDM and having the highest SoC shares the highest power to a ship required with mobile cold-ironing facility whereas the rest of SMGs being within the threshold hold limits, shares the power following their SoCs. Further, it is clarified from Fig. 19 (b) that SoC of SMG_1 and SMG_4 declines the most and the least respectively.

(a) DC-bus voltage and current-sharing among SMGs.

(b) SoC of battery banks in SMGs.

Fig. 20: Experimental results for the case study 4.

4) Case 4: Mobile cold-ironing facility: Lastly, a case study is taken into consideration where all SMGs are within the minimum and maximum threshold limit, i.e., $SoC_{min} \leq SoC_\alpha < SoC_{max}$ and one of the newly berthed ships is connected and is required with the mobile cold-ironing facility. The initial SoC of battery banks in each SMG in this case

are assumed to be $SoC_1 = 35\%$, $SoC_2 = 50\%$, $SoC_3 = 65\%$, and $SoC_4 = 79\%$. It can be inferred from Fig. 20 (a) that the highest current (I_4) is shared by the SMG with higher SoC (SMG_4) and the least current (I_1) is shared by the SMG with lower SoC (SMG_1). Similarly, it can be verified from Fig. 20 (b) that SoC of SMG_1 and SMG_4 decreases the least and the most respectively.

V. Conclusion

In this study, a ships-based seaport microgrid is proposed to provide a mobile cold-ironing facility. This sort of approach is useful where providing a connection from the grid is not deemed as a feasible solution, as building infrastructure for port electrification might not be a cost-effective solution. Further, this approach is particularly beneficial for smaller islands that have a limited source of electricity such as Ærø-island, which only relies on renewable energy resources mainly wind turbines. Moreover, power-sharing among various SMGs based on a communication-less scheme is proposed, which on the basis of SoC of battery banks either absorbs or supply the power. The proposed multi-mode adaptive droop algorithm helps in increasing the lifetime of the battery by not over-charging or over-discharging batteries and to attain SoC balancing in both charging and discharging modes. These modes are VCCM, V-I droop mode, VCDM, and extreme condition modes. In case of an emergency, these interfaced SMGs may support the seaport by providing power from the battery banks, PV, and fuel cell stacks. The economic feasibility and technical challenges including smart metering along with an energy management system of the proposed approach will be addressed in the future study.

References

[1] E. Pastori, "Modal share of freight transport to and from eu ports study," *European Parliament's Committee on Transport and Tourism*, 2015.

[2] Y. V. Fan, S. Perry, J. J. Klemeš, and C. T. Lee, "A review on air emissions assessment: Transportation," *Journal of cleaner production*, vol. 194, pp. 673–684, 2018.

[3] "Mobility and transport." [Online]. Available: https://ec.europa.eu/transport/modes/maritime_en.

[4] M. U. Mutarraf, Y. Terriche, M. Nasir, K. A. K. Niazi, J. C. Vasquez, and J. M. Guerrero, "Hybrid energy storage systems for voltage stabilization in shipboard microgrids," in *2019 9th International Conference on Power and Energy Systems (ICPES)*. IEEE, 2019, pp. 1–6.

[5] O. Merk, "Shipping emissions in ports," 2014.

[6] M. M. Rahim, M. T. Islam, and S. Kuruppu, "Regulating global shipping corporations accountability for reducing greenhouse gas emissions in the seas," *Marine Policy*, vol. 69, pp. 159–170, 2016.

[7] "The european union's maritime transport policy for 2018." [Online]. Available: https://ec.europa.eu/commission/presscorner/detail/de/MEMO_09_16.

[8] K. Stobberup, M. Garza-Gil, A. Stirnemann-Relot, A. Rigaud, N. Franceschelli, and R. Blomeyer, *Research for PECH Committee-Small-scale fisheries and Blue Growth in the EU*, 2017.

[9] Z. Jin, G. Sulligoi, R. Cuzner, L. Meng, J. C. Vasquez, and J. M. Guerrero, "Next-generation shipboard dc power system: Introduction smart grid and dc microgrid technologies into maritime electrical netowrks," *IEEE Electrification Magazine*, vol. 4, no. 2, pp. 45–57, 2016.

[10] M. D. Al-Falahi, T. Tarasiuk, S. G. Jayasinghe, Z. Jin, H. Enshaei, and J. M. Guerrero, "Ac ship microgrids: control and power management optimization," *Energies*, vol. 11, no. 6, p. 1458, 2018.

[11] S. G. Jayasinghe, L. Meegahapola, N. Fernando, Z. Jin, and J. M. Guerrero, "Review of ship microgrids: System architectures, storage technologies and power quality aspects," *inventions*, vol. 2, no. 1, p. 4, 2017.

[12] M. U. Mutarraf, Y. Terriche, K. A. K. Niazi, J. C. Vasquez, and J. M. Guerrero, "Energy storage systems for shipboard microgridsa review," *Energies*, vol. 11, no. 12, p. 3492, 2018.

[13] N. B. B. Ahamad, J. M. Guerrero, C.-L. Su, J. C. Vasquez, and X. Zhaoxia, "Microgrids technologies in future seaports," in *2018 IEEE International Conference on Environment and Electrical Engineering and 2018 IEEE Industrial and Commercial Power Systems Europe (EEEIC/I&CPS Europe)*. IEEE, 2018, pp. 1–6.

[14] K. Mahmud, M. S. Rahman, J. Ravishankar, M. J. Hossain, and J. M. Guerrero, "Real-time load and ancillary support for a remote island power system using electric boats," *IEEE Transactions on Industrial Informatics*, vol. 16, no. 3, pp. 1516–1528, 2019.

[15] C.-H. Cheng, P.-J. Cheng, and M.-J. Xie, "Current sharing of paralleled dc–dc converters using ga-based pid controllers," *Expert Systems with Applications*, vol. 37, no. 1, pp. 733–740, 2010.

[16] A. P. Martins, A. S. Carvalho, and A. Araujo, "Design and implementation of a current controller for the parallel operation of standard upss," in *Proceedings of IECON'95-21st Annual Conference on IEEE Industrial Electronics*, vol. 1. IEEE, 1995, pp. 584–589.

[17] S. K. Mazumder, M. Tahir, and K. Acharya, "Master–slave current-sharing control of a parallel dc–dc converter system over an rf communication interface," *IEEE Transactions on Industrial Electronics*, vol. 55, no. 1, pp. 59–66, 2008.

[18] T.-F. Wu, Y.-K. Chen, and Y.-H. Huang, "3c strategy for inverters in parallel operation achieving an equal current distribution," *IEEE Transactions on Industrial Electronics*, vol. 47, no. 2, pp. 273–281, 2000.

[19] J. M. Guerrero, J. C. Vasquez, J. Matas, L. G. De Vicuña, and M. Castilla, "Hierarchical control of droop-controlled ac and dc microgrids–a general approach toward standardization," *IEEE Transactions on industrial electronics*, vol. 58, no. 1, pp. 158–172, 2010.

[20] X. Lu, K. Sun, J. M. Guerrero, J. C. Vasquez, L. Huang, and R. Teodorescu, "Soc-based droop method for distributed energy storage in dc microgrid applications," in *2012 IEEE International Symposium on Industrial Electronics*. IEEE, 2012, pp. 1640–1645.

[21] X. Lu, K. Sun, J. M. Guerrero, J. C. Vasquez, and L. Huang, "State-of-charge balance using adaptive droop control for distributed energy storage systems in dc microgrid applications," *IEEE Transactions on Industrial electronics*, vol. 61, no. 6, pp. 2804–2815, 2013.

[22] M. Nasir, Z. Jin, H. A. Khan, N. A. Zaffar, J. C. Vasquez, and J. M. Guerrero, "A decentralized control architecture applied to dc nanogrid clusters for rural electrification in developing regions," *IEEE Transactions on Power Electronics*, vol. 34, no. 2, pp. 1773–1785, 2018.

[23] Z. Jin, L. Meng, and J. M. Guerrero, "Comparative admittance-based analysis for different droop control approaches in dc microgrids," in *2017 IEEE Second International Conference on DC Microgrids (ICDCM)*. IEEE, 2017, pp. 515–522.

[24] F. Gao, S. Bozhko, A. Costabeber, C. Patel, P. Wheeler, C. I. Hill, and G. Asher, "Comparative stability analysis of droop control approaches in voltage-source-converter-based dc microgrids," *IEEE Transactions on Power Electronics*, vol. 32, no. 3, pp. 2395–2415, 2016.

[25] M. Nasir, M. Anees, H. A. Khan, and J. M. Guerrero, "Dual-loop control strategy applied to the cluster of multiple nanogrids for rural electrification applications," *IET Smart Grid*, vol. 2, no. 3, pp. 327–335, 2019.

[26] M. Nasir, H. A. Khan, K. A. K. Niazi, Z. Jin, and J. M. Guerrero, "Dual-loop control strategy applied to pv/battery-based islanded dc microgrids for swarm electrification of developing regions," *The Journal of Engineering*, vol. 2019, no. 18, pp. 5298–5302, 2019.

[27] M. U. Mutarraf, Y. Terriche, M. Nasir, Y. Guan, C.-L. Su, J. C. Vasquez, and J. M. Guerrero, "A decentralized control scheme for adaptive power-sharing in ships based seaport microgrid." in *IECON 2020 The 46th Annual Conference of the IEEE Industrial Electronics Society*. IEEE, 2020, pp. 3126–3131.

[28] Q. Shafiee, T. Dragičević, J. C. Vasquez, and J. M. Guerrero, "Hierarchical control for multiple dc-microgrids clusters," *IEEE Transactions on Energy Conversion*, vol. 29, no. 4, pp. 922–933, 2014.

[29] A. Burkov and G. Y. Kuvshinov, "Study of ships electrification," in *2017 International Conference on Industrial Engineering, Applications and Manufacturing (ICIEAM)*. IEEE, 2017, pp. 1–6.